Bounded Homotopy with four solution lines applied to nonlinear circuit simulation

Héctor Vázquez-Leal
Universidad Veracruzana
Facultad de Instrumentación Electrónica
Xalapa, Veracruz, México
Email: hvazquez@uv.mx

Luis Hernández-Martínez
INAOE
Departamento de Electrónica
Email: luish@inaoep.mx

Arturo Sarmiento-Reyes
INAOE
Departamento de Electrónica
Email: jarocho@inaoep.mx

Roberto Castañeda Sheissa
Universidad Veracruzana
Facultad de Instrumentación Electrónica
Xalapa, Veracruz, México
Email: rocastaneda@uv.mx

Abstract

This work shows a new double bounded Homotopy based on a polynomial formulation with four lines separated by a fixed distance. The new Homotopy scheme presents a bounding between the two internal solution lines and the symmetry axis, which allows to establish a stop criterion for the simulation. Besides, the initial and final points on this new double bounded Homotopy can be set arbitrarily. New mathematical properties fo the new Homotopy will be introduced and be exemplified by means of some mathematical and circuital cases.

I. INTRODUCTION

The electronic industry, so demanding and competitive as well, constantly pushes circuit's area to the limit of the human knowledge. This has created an accelerated growing on the integration leves for the integrated circuits (IC). In [5] Moore's Law is introduced which describes the exponential growing on the integrated circuits density, reaching the 2 billion transistors within a single integrated circuit in 2008. Thus the need to develop software tools to simulate the circuit performance that every day is becoming more complex. In particular, the Homotopy has direct impact in simulation tools for ICs, and in general into any science area where a phenomenon can be modelled using non-linea equation systems. The reason that one given circuit could have more than one operating point in DC and the way to solve such points are solved using Homotpy methods [10].

The task to find the DC solution is important because this analysis is the starting point fot the rest of the common test regularly done through the circuit design process (for instance, small-signal analysis). This analysis consists in finding the solutions for a non-linear equation system (NAEs) from the ICs [13], [12]. These NAEs becomes complex due to the accelerated increase of the transistores employed in the IC and by the use of complex models used (as a result of reducing the components dimensions) causing two phenomena: existence of multiple unexpected operating points and convergence failures for the Newton-Raphson (NR) method). The NR method is employed by the majority of the integrated circuit simulators. The reason for the widespread use of the Newton method is its quadratic convergence rate which reduce the computing times for the simulations. Nevertheless, the Newton method suffers some convergence issues [4], [13] which are described by cases in figure 1 where $f(x)$ is the equation to be solved.

- **Case** A Can be observed how the method converge to a single solution. This method is locally convergent [13] because if the initial point es not close enough to the solution, the method could fail.
- **Case** B In this case the method oscillates in certain region because is based in a functioning principle based in curve tangents for the $f(x)$ curve. It also shows how the initial point selection can affect, radically, the method's convergence. The oscillation is produced by an undetermined arbitrarily number of iterations set to limit each simulation, once this number is reached the simulation is stopped throwing a convergence error; this situation serves the base to use alternative methods to find solutions.

- **Case** C Here can be seen the way the method converges to another solution. The choice to select a different initial point may lead to locate another solution but this method is unable to locate more than one solution by simulation.
- **Case** D This case diverges given its functioning nature based on tangents to the cruve $f(x)$. The divergence produces high values on variables which can be translated in numerical overflow that cause failures and simulation to be finalized.
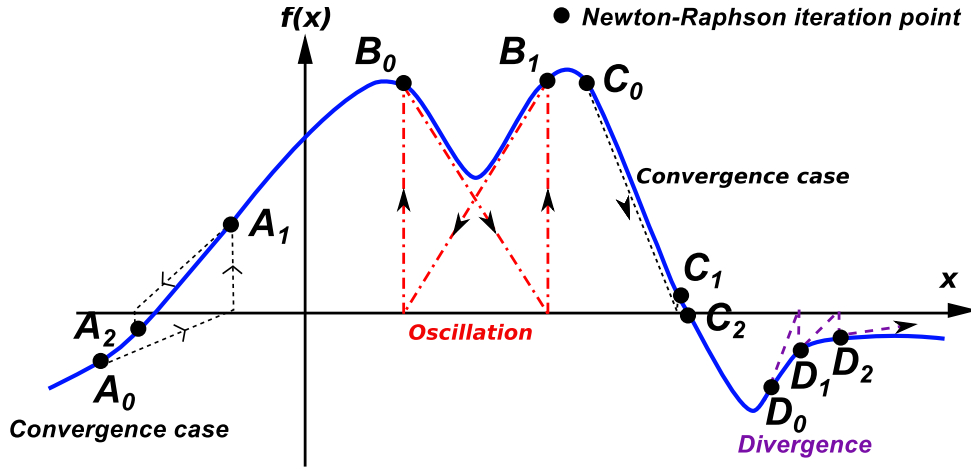

Fig. 1: Newton-Raphson convergence and divergence cases.

Convergence problems (cases B and D) for the NR method becomes more difficult as the complexity of equations increase due by the high non-linearities present. In fact, the NR method was used since the development for the first integrated circuit simulator SPICE [1] in 1975, by that time the densest circuits included about 10,000 transistor by IC, which notoriously contrasts with the more than 2 billion transistors [5] that a modern IC can contain; this is a huge growth on size and complexity for the problem to be solved by Newton's method. Besides to the increase on the number of transistors, the complexity of the physical models which describe the behavior of current transistors (because being of sub-micron dimensions means more complex physical behaviors [7]).

The ERDD circuit in figure 2 contains the following series setting: two tunnel diodes (K3 and K4), one resistor (R2), and a voltage source (V1).
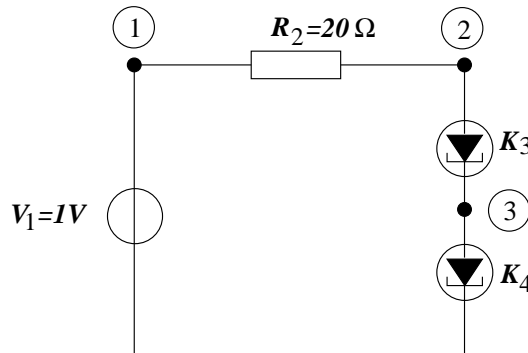

Fig. 2: Two tunnel diodes circuit.

Both tunnel diodes are identical showing the following branch function:

$$i = I_p(\frac{V}{V_p})e^{1-\frac{V}{V_p}} + I_0 e^{\frac{q}{KT}V}$$

where the value for the voltage source V_1 is $1V$ and for resistor R_2 is 20Ω. Besides, both tunnel diodes (K_3 and K_4) have the same model with coefficients: $Ip = 100 \times 10^{-3}$, $V_p = 50 \times 10^{-3}$, $I_0 = 1 \times 10^{-9}$ y $\frac{q}{KT} = 40$.

```
Direct Newton iteration failed to find .op point.  (Use ".option noopiter" to skip.)
Gmin steping method for .op point skipped.
Starting source stepping with srcstepmethod=0
Source Step = 3.0303%
Source Step = 33.3333%
Source Step = 63.6364%
Source Step = 93.9394%
Source stepping succeeded in finding the operating point.


Date: Mon Jan 25 11:16:08 2010
Total elapsed time: 0.016 seconds.
```

Fig. 3: Error message for the Newton-Raphson method in LTSPICE IV.

This circuit has a total of 9 operating points or solutions, from which integrated circuit simulators are capable to locate one solution, at best. The former can be exemplified using the simulator LTSpice IV [8] to perform a DC analysis for the circuit shown in figure 3. The chosen starting point is $v_1 = v_2 = v_3 = v_4 = 2V$ for the NR method. The result is shown in figure 3, it is caused by a convergence failure on the NR method (Direct Newton iteration failed to find .op point). This is a serious event for the NR method since the circuit contains just 4 transistors compared to commercial circuits that can contain millions or billions (this is a huge increase on the complexity of the equilibrium equation). Once the NR method fails, the simulator executes automatically a back-up numerical method called conductance staggering [2], [1], [3], which finds one operating point. In fact, the conductance staggering is a primitive type of Homotopy classified as natural type Homotopy.

Circuit designers face convergence failures commonly using the NR method and back-up methods, thus, as last resort, the modification of some parameters of the numerical engine are enforced expecting to reach convergence. This situation increase design times, making the entire design cycle slow and expensive. This situation, by itself, justifies the use of alternative methods to Newton like Homotopy to locate the operating point. Nevertheless, there are more reasons to use Homotopy methods like the existence of multiple operating points. This is because, unlike Newton, Homotopy is capable to locate multiple operating points. This is important because it is possible that the designer could approve certain DC operating point (found by the Newton method) that may not be physically present in the already fabricated IC. This is translated in malfunctioning of the circuit which could, in the end, represent high loses for the company in financial terms.

Homotopy methods [11], [18], [6], [19], [9] have been proved as useful to locate multiple operating points and converge to solutions where the Newton method does not. Nevertheless, Homotopy methods are affected by certain inconveniences, among them are: stop criterion and computing time.

II. DOUBLE BOUNDED HOMOTOPY

Considering the existance of two solution lines, one at $\lambda = a$ and the other at $\lambda = b$ the Homotopy formulation is the following:

$$\boldsymbol{H}(\boldsymbol{f}(\boldsymbol{x}), \lambda) = \boldsymbol{0} \tag{1}$$

where λ is the Homotopy variable and $\boldsymbol{H}^{-1}(\boldsymbol{0})$ the family of solutions that makes up the Homotopy path, such that:

- For $\lambda = 0.5(a + b)$ the solution for $H^{-1}(.)$ is known or easy to obtain, in computer terms. This point is known as the initial point for the Homotopy (λ_i).
- As for $\lambda = a$, $\boldsymbol{H}(\boldsymbol{f}(\boldsymbol{x}), a) = \boldsymbol{f}(\boldsymbol{x})$. Means that at $\lambda = a$ all solutions for $\boldsymbol{f}(\boldsymbol{x})$ are placed.
- For $\lambda = b$, $\boldsymbol{H}(\boldsymbol{f}(\boldsymbol{x}), b) = \boldsymbol{f}(\boldsymbol{x})$. Means that at $\lambda = b$ all solutions for $\boldsymbol{f}(\boldsymbol{x})$ are placed.
- The path for $\boldsymbol{H}^{-1}(\boldsymbol{0})$ is a continuous function for λ in the range of $a \leq \lambda \leq b$.

III. DOUBLE BOUNDED POLYNOMIAL HOMOTOPY WITH FOUR SOLUTION LINES

The double bounded polynomial Homotopy with 4 solution lines (DBP4) is defined by this equation:

$$\boldsymbol{H}(\boldsymbol{f}(\boldsymbol{x}), \lambda) = Q(x - x_i)(x - x_f) + C(\lambda - a/2)^2 \boldsymbol{f}(\boldsymbol{x})^2 \tag{2}$$
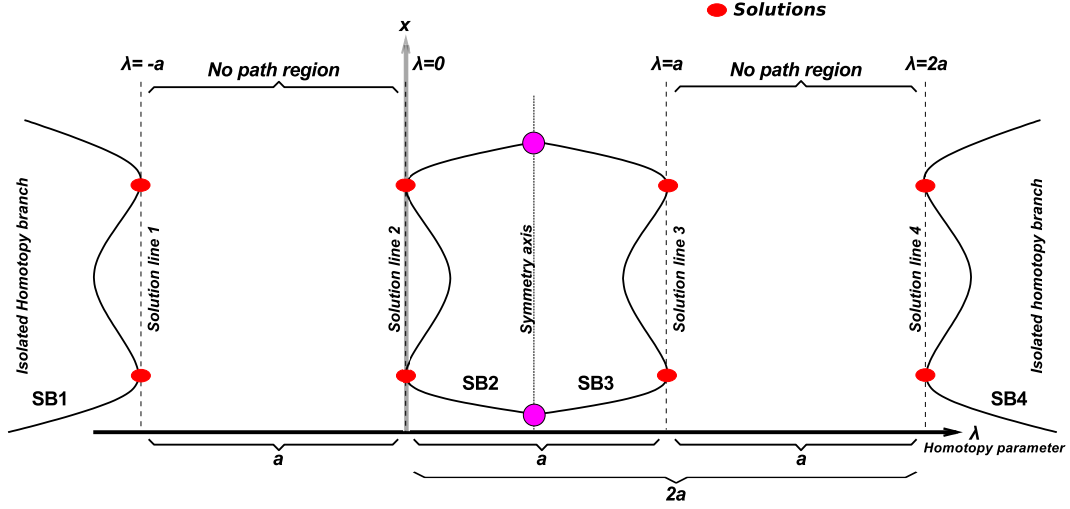
Fig. 4: General scheme for polynomial Homotopy with double solution.

where $Q = \lambda(\lambda + a)(\lambda - a)(\lambda - 2a)$, a is a constant that represents separation between solution lines, x_i is the initial point, x_f the final point, and C an arbitrary constant.

Based on the previous, Homotopy can be expressed in general way as:

$$\boldsymbol{H}(\boldsymbol{f}(\boldsymbol{x}), \lambda) = \begin{cases} f(x^*) = 0 & \text{for } \lambda = 0 \text{ y } x = x^* \\ (x - x_i)(x - x_f) = 0 & \text{for } \lambda = a/2 \\ f(x^*) = 0 & \text{for } \lambda = a \text{ y } x = x^* \end{cases}$$

where x^* is any solution for $f(x)$, x_i and x_f are Homotopy's initial and final points, respectively.

This Homotopy contains 4 solution lines ($\lambda = -a$, $\lambda = 0$, $\lambda = a$, and $\lambda = 2a$). Nevertheless, the two solution lines for both ends are unconnected branches not used for tracing purposes. Squaring the function $f(x)$ has the finality to establish an even number of solutions (or operating points) which precisely produces the bounding and closes the Homotopy path inside the middle region.

Figure 5 shows how Homotopy path starts at $A = (x_i, a/2)$ on the symmetry axis, finds two roots (in region $SB3$) and finishes when a new crossing through the symmetry axis at $B = (x_f, a/2)$ is detected, which means that tracing for a symmetrical branch has been completed and fulfilling the stop criterion.
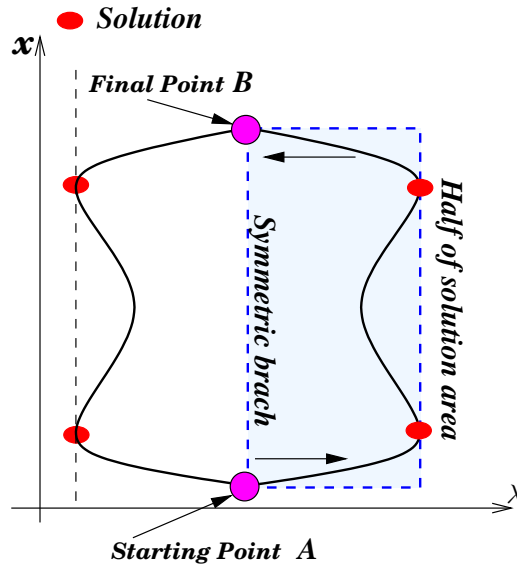

Fig. 5: Stop criterion.

The properties for this new Homotopy are presented in the following sub-sections:

Symmetry branch	Formulation	Limit at $f(x^*) = 0$
SB1	$\lambda_1 = \frac{a - \sqrt{5\,a^2 + 2\,\sqrt{(J(x)+4\,a^2)(J(x)+a^2)} + 2\,J(x)}}{2}$	$\lambda = -a$
SB2	$\lambda_2 = \frac{a - \sqrt{5\,a^2 - 2\,\sqrt{(J(x)+4\,a^2)(J(x)+a^2)} + 2\,J(x)}}{2}$	$\lambda = 0$
SB3	$\lambda_3 = \frac{a + \sqrt{5\,a^2 - 2\,\sqrt{(J(x)+4\,a^2)(J(x)+a^2)} + 2\,J(x)}}{2}$	$\lambda = a$
SB4	$\lambda_4 = \frac{a + \sqrt{5\,a^2 + 2\,\sqrt{(J(x)+4\,a^2)(J(x)+a^2)} + 2\,J(x)}}{2}$	$\lambda = 2a$

TABLE I: Symmetrical branches

A. Symmetrical branches

To obtain the branches for the Homotopy path, first the equation 2 is reformulated as follows:

$$\boldsymbol{H}(\boldsymbol{f}(\boldsymbol{x}), \lambda) = \lambda(\lambda + a)(\lambda - a)(\lambda - 2a) + (\lambda - a/2)^2 J(x) = 0 \tag{3}$$

where

$$J(x) = \frac{Cf(x)^2}{(x-x_i)(x-x_f)}$$

Symmetrical branches shown in figure 4 can be derived solving λ from equation 3. The result is 4 symmetrical branches. Each branch *SB1, SB2, SB3*, and *SB4* is linked to a different solution line $\lambda = [-a, 0, a, 2a]$, respectively. In order to trace the Homotopy path, the unconnected symmetrical paths *SB1* and *SB4* will be ignored because these open branches would make not possible to apply the stop criterion. Given the fact that *SB2* and *SB3* are connected and symmetrical, only one can be traced to obtain the full path and finalize the simulation. *SB3* is chosen as the tracing path, which touches obliquely the solution line $\lambda = a$.

B. Symmetry axis

The symmetry axis is an important property for the double bounded Homotopy. In the particular case of the polynomial double bounded Homotopy the symmetry axis is:

$$\lambda_{sym} = \frac{a}{2} \tag{4}$$

This symettry axis belong to the symmetry relationship between $SB2$ and $SB3$ branches.
As shown in figure 6, this relationship must be fulfilled:

$$\lambda_3 - \lambda_{sym} = \lambda_{sym} - \lambda_2$$

Replacing the value for λ_{sym}, we obtain:

$$\lambda_3 - 0.5a = 0.5a - \lambda_2$$

Then, replacing λ_2 and λ_3 for their respective functions the next relationship is found:

$$0.5a + 0.5\sqrt{G(\boldsymbol{x})} - 0.5a = 0.5a - 0.5a + 0.5\sqrt{G(\boldsymbol{x})}$$

where $G(\boldsymbol{x}) = \sqrt{5\,a^2 - 2\,\sqrt{(J(x) + 4\,a^2)(J(x) + a^2)}}$
Reducing terms:

$$0.5\sqrt{G(\boldsymbol{x})} = 0.5\sqrt{G(\boldsymbol{x})}$$
$$0 = 0$$

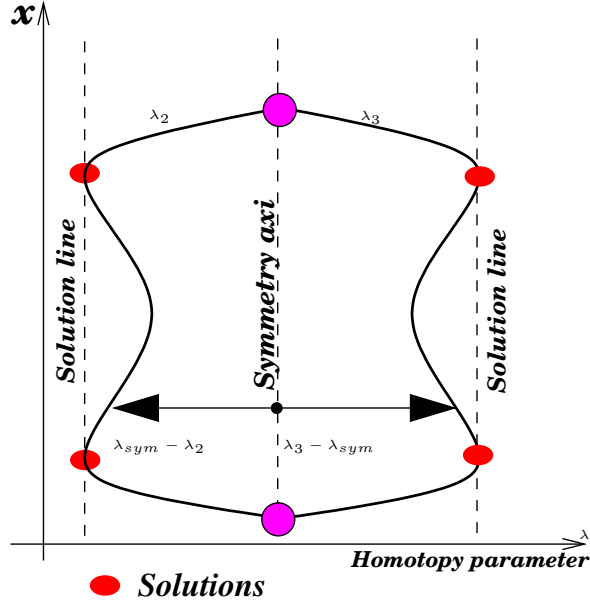The proof for this equality shows that the Homotopy path is symmetrical around the symmetry axis.

Fig. 6: Symmetry of the Homotopy path.

C. Initial point and final point

The point where the Homotopy path starts is located right on the symmetry axis, therefore $\lambda_i = a/2$. Thus, replacing λ_i in equation 2 cancels the term that contains the equilibrium equation $f(x)$, achieving:

$$\boldsymbol{H}(\boldsymbol{f}(\boldsymbol{x}), \lambda_i) = (x - x_i)(x - x_f) = 0$$

Therefore, the initial point x_i and final point x_f are chosen arbitrarily.

Solving for λ in equation 2 the branch SB3 is:

$$\lambda_3 = \frac{Fa + \sqrt{5\,F^2a^2 - 2\,F\sqrt{4\,F^2a^4 + 5\,F\,(f\,(x))^2\,a^2 + (f\,(x))^4} + 2\,F\,(f\,(x))^2}}{2F}$$

where $F = (x - x_i)(x - x_f)$. Now, the following limits are calculated:

$$\lim_{x \to x_i} \lambda_3 = 0.5a \tag{5}$$

$$\lim_{x \to x_f} \lambda_3 = 0.5a \tag{6}$$

Hence, when x tends to the value for the initial point x_i or final point x_f, the Homotopy parameter λ tends to the symmetry axis at $\lambda = 0.5a$.

D. Circuital rendering

The circuital rendering for the double bounded Homotopy can be derived solving $f(x)$ from the Homotopy expression in equation 2. From former equation can be concluded that there are non-linear current sources (K_1, ,K_n) connected to every node of the circuit, where n is the number of nodes, and I the number of constant voltage sources (E).

$$I_{K_i} = \frac{\lambda(\lambda + a)(\lambda - a)(\lambda - 2a)(V_{xk} - V_{xk_i})(V_x - V_{xk_f})}{(\lambda - a/2)^2} \tag{7}$$

where $k = [1, n]$, V_{xk} are the nodal voltages of the circuit, V_{xk_i} and V_{xk_f} are constant values related to the initial and final points for each variable V_{xk} in the Homotopy. Finally, the circuital rendering of the Homotopy at the symmetry axis can be seen in figure 7.
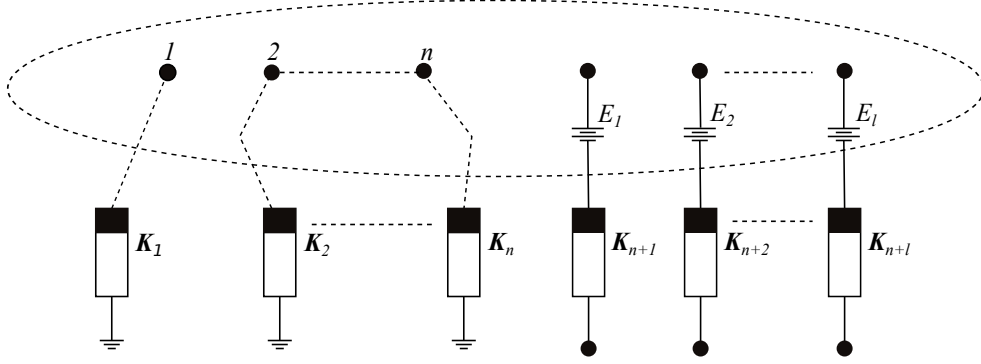
Fig. 7: Circuital rendering for the double bounded Homotopy.

E. Multiple variables

When Homotopy is applied to a non-linear equation system with multiple variables, the generalization is given by:

$$H_1(f_1(x), \lambda) = Q(x_1 - x_i)(x_1 - x_f) + C(\lambda - a/2)^2 f_1(x)^2$$

$$H_2(f_2(x), \lambda) = Q(x_2 - x_i)(x_2 - x_f) + C(\lambda - a/2)^2 f_2(x)^2$$

$$H_3(f_3(x), \lambda) = Q(x_3 - x_i)(x_3 - x_f) + C(\lambda - a/2)^2 f_3(x)^2$$

$$\vdots \qquad\qquad \vdots \qquad\qquad \vdots$$

$$H_n(f_n(x), \lambda) = Q(x_n - x_i)(x_n - x_f) + C(\lambda - a/2)^2 f_n(x)^2$$

where n is the number of equations of the equilibrium equation $\boldsymbol{f}(x)$, f_i represents every nodal equations or extra equations for non-NA compatible elements [12], C is an arbitrary constant, and $Q = \lambda(\lambda + a)(\lambda - a)(\lambda - 2a)$.

Figure 8 presents a polygon showing in a descriptive way the behavior of the possible Homotopy paths staring from different initial points, result of combining the initial and final points for every x. Therefore, each vertex represents the possible start or ending for the Homotopy path. Next, some possible cases are described. The total number of vertexes for the polygon is n^2.

- In the case of point p_1 the Homotopy path ends at p_5, crossing through 3 operating points (S_1, S_2, y S_3).
- For point p_2 the Homotopy path ends at p_4, crossing through 2 operating points (S_2 and S_3), which are common to the path described by $p_1 - p_5$.
- For the case of point p_3 the Homotopy path ends at $p_{(n^2)}$, crossing through 3 operating points (S_1, S_2, and S_3), which are common to the path described by $p_1 - p_5$.

F. Curvature radius

The curvature radius for the Homotopy path will be employed as an analysis tool *cualitativamente* of the paths on strategic points like solutions and turning points (see figure 9). Curvature radius for a curve in a point is the radius for a circle with curvature equivalent at that point of the curve.

The equation for the curvature radius is:

$$\rho = \left| \frac{(1 + (y')^2)^{3/2}}{y''} \right|$$

where y is a function $y(x)$, y' is the first derivative of $y(x)$ with respect to x and y'' is the second derivative of $y(x)$ with respect to x. In terms of the Homotopy path, the first derivative y' is equal to $\frac{d\lambda}{dx}$ and the second derivative y'' is equal to $\frac{d^2\lambda}{dx^2}$.

The slope of the Homotopy path at the solution points and turning points is zero ($y' = \frac{d\lambda}{dx} = 0$), property that can be used to simpplify the expression for the curvature radius in those points, like:

$$\rho = \left| \frac{1}{\frac{d^2\lambda}{dx^2}} \right|$$

Now, λ_3 from equation SB3 in table I is derived twice with respect to x and considering a and C as constants. Next, $f(x)$ is replaced by zero because it is the solution point, we obtain:

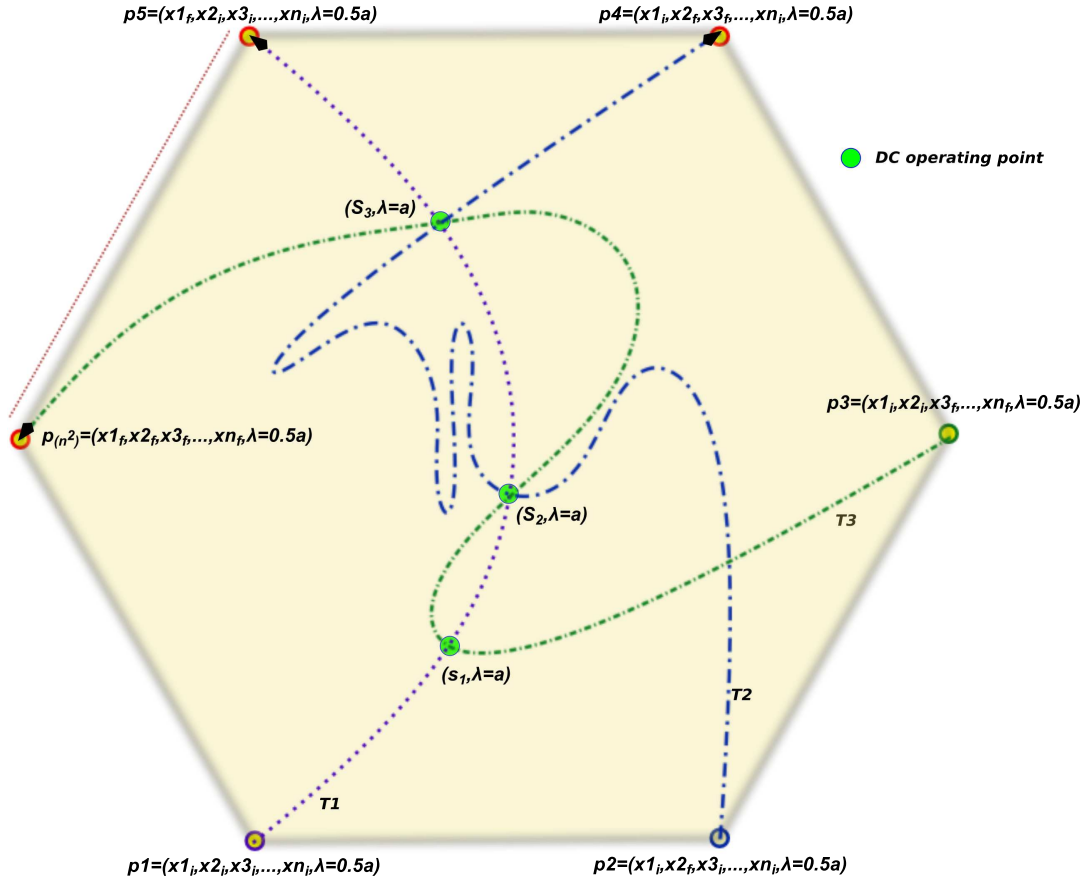$$\rho_s = \left[4 \frac{a(x - x_i)(x + x_f)}{C\left(\frac{d}{dx} f(x)\right)^2} \right]_{x = x_s}$$

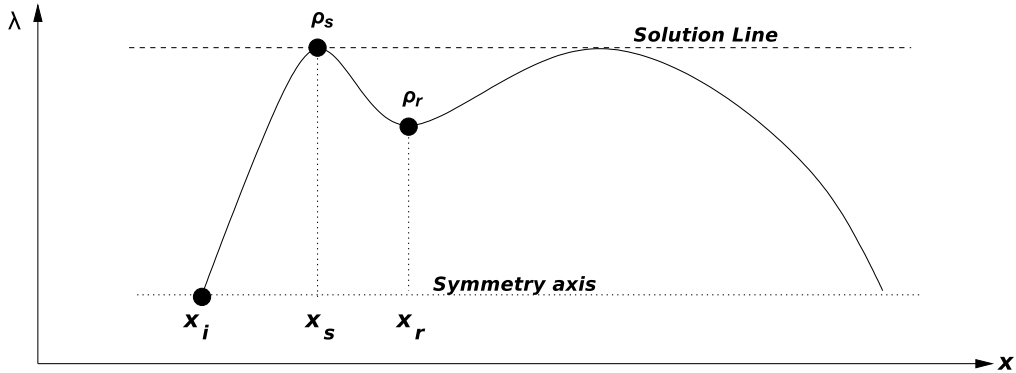Fig. 8: Initial and final points vertexes for the Homotopy path.

Fig. 9: Solution point ρ_s and turning point ρ_r

where x_s is the value of the solution and a represents the separation between solution lines.

The equation ρ_s allows to conclude that distance a between solution lines affects the sharpness of the Homotopy path on the solutions, in such a way that the curve is more acute as solution lines approach (each other) and flattens as solution lines distance each other. Besides, constant C also affects the curve, flattening on the solution when$C$ increases and more acute as C decreases.

The point where path returns to the solution search is called turning point ρ_r. The study of the curvature radius at the turning point ρ_r complements with the study of the curvature radius at solutions ρ_s in order have a deeper understanding of the qualitative behavior of the Homotopy path. At the turning point, the derivative of λ with respect to x equals zero. Besides, the turning point spatially matches the critical points of function $f(x)$, thus the derivative of $f(x)$ with respect to x is zero.

In order to simplify the equation for the curvature radius it is assumed that:

$$j(x) = \frac{f(x)^2}{(x-x_i)(x-x_f)}$$

Therefore, the equation for the curvature radius is:

$$\rho_r = \left[\frac{4\sqrt{5\,a^2 - 2\sqrt{4\,a^4 + 5\,Cj\,(x)\,a^2 + C^2\,(j\,(x))^2} + 2\,Cj\,(x)}}{\left(-\frac{5\,C\left(\frac{d^2}{dx^2}j(x)\right)a^2 + 2\,C^2 j(x)\frac{d^2}{dx^2}j(x)}{\sqrt{4\,a^4 + 5\,Cj(x)a^2 + C^2(j(x))^2}} + 2\,C\frac{d^2}{dx^2}j\,(x) \right)} \right]_{x=x_r}$$

where x_r is the value for x at the turning point.

To evaluate qualitatively the behavior of the curvature radius is necessary to carry out the following symbolic limits:

$$\lim_{f(x)\to+\infty} |\rho_r| = \infty \tag{8}$$

$$\lim_{f(x)\to+0} |\rho_r| = \left[8\,\frac{a}{C\frac{d^2}{dx^2}f\,(x)} \right]_{x=x_r} \tag{9}$$

The limit for equation 8 shows that when $f(x)$ tends to high values, the curvature radius grows, leaving the curve flat. When $f(x)$ has high values (evaluated at turning point x_r) is fairly common on the nodal equations of the circuit. Therefore, the Homotopy path will tend to stay close to the solution line $\lambda = a$. Suppose that a polynomial double bounded Homotopy is solved with $a = 1$. In figure 10(a) is shown the symmetric branch located at the right corresponding to $\lambda = 1$. In the latter figure is difficult to differentiate between solutions and turning points. Closing-up to the solution line at $\lambda = 1$ (see figura 10(b)) allows to appreciate the solutions and turning points. This phenomenon was checked simulating various circuits and non-linear equations. The limit for equation 9 indicates that when $f(x)$ tends to small values, the curvature radius es proportional to the value for solution line a and inversely proportional to constant C.
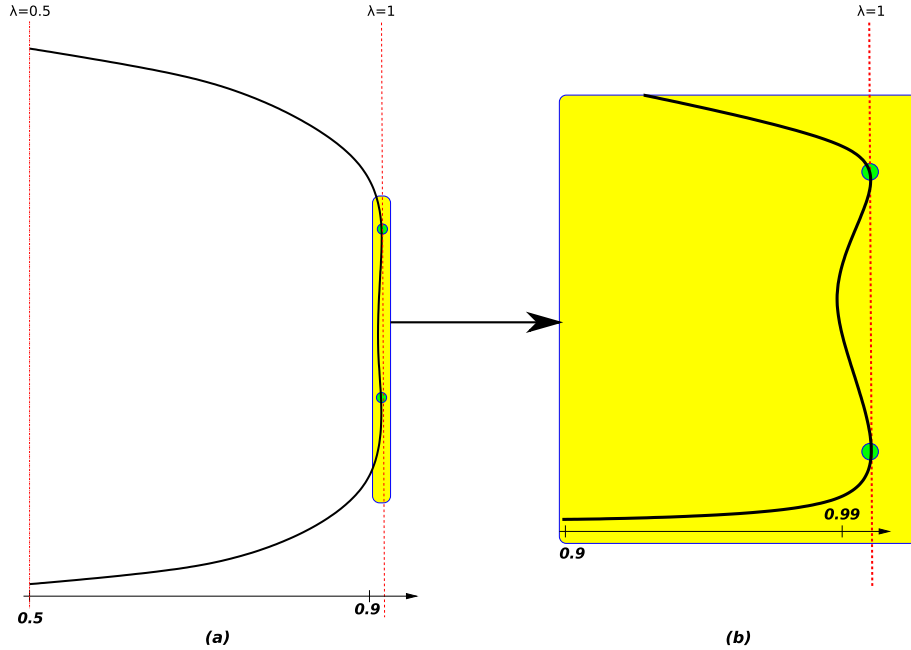

Fig. 10: a) Homotopic path. b) Close-up to the solutions region.

IV. STUDY CASES

Double bounde Homotopy has been developed to simulate non-linear circuits with multiple solutions. This section will show Homotopy simulations on several types of circuits to expose the new proposed method to a variety of non-linear functions.

A. Mathematical case

To show the use of Homotopy for a two-dimensional example, Homotopy is applied to the following NAEs system:

$$f_1(x_1, x_2) = (x_2 - 1)(x_2 - 4)(x_2 - 6) + x_1 = 0$$
$$f_2(x_1, x_2) = (x_1 - 3)(x_1 - 6)(x_1 - 9) + x_2 = 0$$

Graphical solution of the system is shown in figure 11.
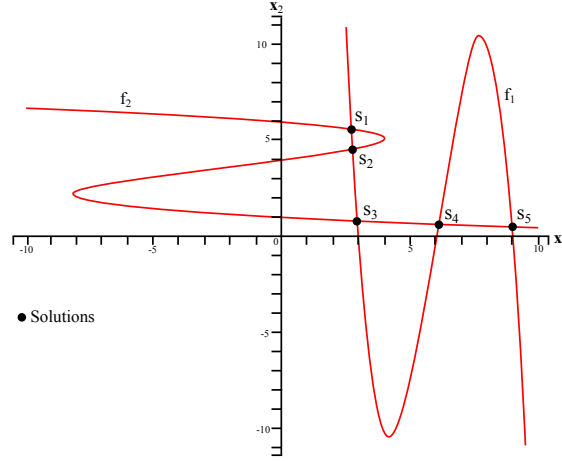The proposed Homotopy formulation is:

Fig. 11: Five solution system.

$$H_1(f_1, \lambda) = \lambda(\lambda + 1)(\lambda - 1)(\lambda - 2)(x_1 - 13)(x_1 + 13) + (\lambda - 0.5)^2 f_1^2 = 0$$
$$H_2(f_2, \lambda) = \lambda(\lambda + 1)(\lambda - 1)(\lambda - 2)(x_2 - 13)(x_2 + 13) + (\lambda - 0.5)^2 f_2^2 = 0$$

where the solution line es placed at $\lambda = 0$ and $\lambda = 1$. For practical purposes, just the symmetrical branch for the Homotopy path linked to solution line $\lambda = 1$ is plotted.

Initial point is chosen as $A = [x_1 = -13, x_2 = -13]$ and tracing of the path is started, resulting in a global convergence to all the solutions of the system (S_1, S_2, S_3, S_4 and S_5) (see figure 12). Final point is $B = [x_1 = 13, x_2 = 13]$ and the Homotopy path for each variable ($x_1 - \lambda$ and $x_2 - \lambda$) are shown in figures 13a and 13b.

B. Circuit with two tunnel diodes

Tunnel diodes have non-linear behavior, which can be depicted in general way in figure 14a. As it can be seen, tunnel diode has three sign changes on the slope which combined with a load line could produce up to three solutions per tunnel diode present in the circuit. In this example, the model chosen for the tunnel diode is a function of exponential terms [15],[14] and can be expressed as:

$$i = I_p\left(\frac{V}{V_p}\right)e^{1 - \frac{V}{V_p}} + I_0 e^{\frac{q}{KT}V}$$

Exponential terms can produce numerical overflows, thus this circuit represents a challenge for the double bounded Homotopy. Hence, in this example an ERDD circuit is presented; consists of 2 tunnel diodes, a voltage source, and a resistor all of them connected in series (see figure 14b). The voltage source V_1 has the value $1V$ and the resistor R_2 is 20Ω. Besides, both tunnel diodes (K_3 and K_4) have the same model with coefficients: $Ip = 100 \times 10^{-3}$, $V_p = 50 \times 10^{-3}$, $I_0 = 1 \times 10^{-9}$ y $\frac{q}{KT} = 40$. The equilibrium equation is formulated form the modified nodal analysis of the circuit. Besides, the system is reduced to three equations eliminating the nodal voltage v_1 because its constant and equal to the voltage source value. Therefore, variables taken into account are: I_E, v_2, and v_3. Equations are expressed as:

$$f_1 = \frac{1}{20} - \frac{v_2}{20} + I_E = 0$$

$$f_2 = -\frac{1}{20} + \frac{v_2}{20} + 2(v_2 - v_3)e^{(1 - 20v_2 + 20v_3)}$$
$$+ 1 \times 10^{-9} e^{(40v_2 - 40v_3)} = 0$$

$$f_3 = 2(v_2 - v_3)e^{(1 - 20v_2 + 20v_3)} + 1 \times 10^{-9} e^{(40v_2 - 40v_3)}$$
$$- 2v_3 e^{(1 - 20v_3)} - 1 \times 10^{-9} e^{(40v_3)} = 0$$

Now, DBH is applied to solve the circuit, the Homotopy formulation is expressed as follows:

$$H_1(f_1, \lambda) = \lambda(\lambda + 1)(\lambda - 1)(\lambda - 2)(I_E - 1)(I_E + 1) + (\lambda - 0.5)^2 f_1^2 = 0$$
$$H_2(f_2, \lambda) = \lambda(\lambda + 1)(\lambda - 1)(\lambda - 2)(v_2 - 1)(v_2 + 1) + (\lambda - 0.5)^2 f_2^2 = 0$$
$$H_3(f_3, \lambda) = \lambda(\lambda + 1)(\lambda - 1)(\lambda - 2)(v_3 - 1)(v_3 + 1) + (\lambda - 0.5)^2 f_3^2 = 0$$

where bounding lines are $a = 0$ and $b = 1$, and initial point for the Homotopy path is selected at $A = [I_E = -1, v_2 = -1, v_3 = -1]$.

As result for the Homotopy tracing all the operating points were located, 9 points in total. Also, the final point for the path is located at $B = [I_E = 1, v_2 = 1, v_3 = 1$. Figure 15(b) shows a close-up to the solutions region, here can be seen how the path crosses through the 9 solutions, presenting 3 sub-regions ($F1$, $F2$ y $F3$). In order to observe in detail the behavior of the path, an enlargement for each one of the regions $F1$, $F2$, and $F3$ is also shown (see figuras 15(c), 15(d), and 15(e)). In these figures all 9 solutions ($S_1, S_2, S_3, S_4, S_5, S_6, S_7, S_8$ y S_9) are shown on the Homotopy path.
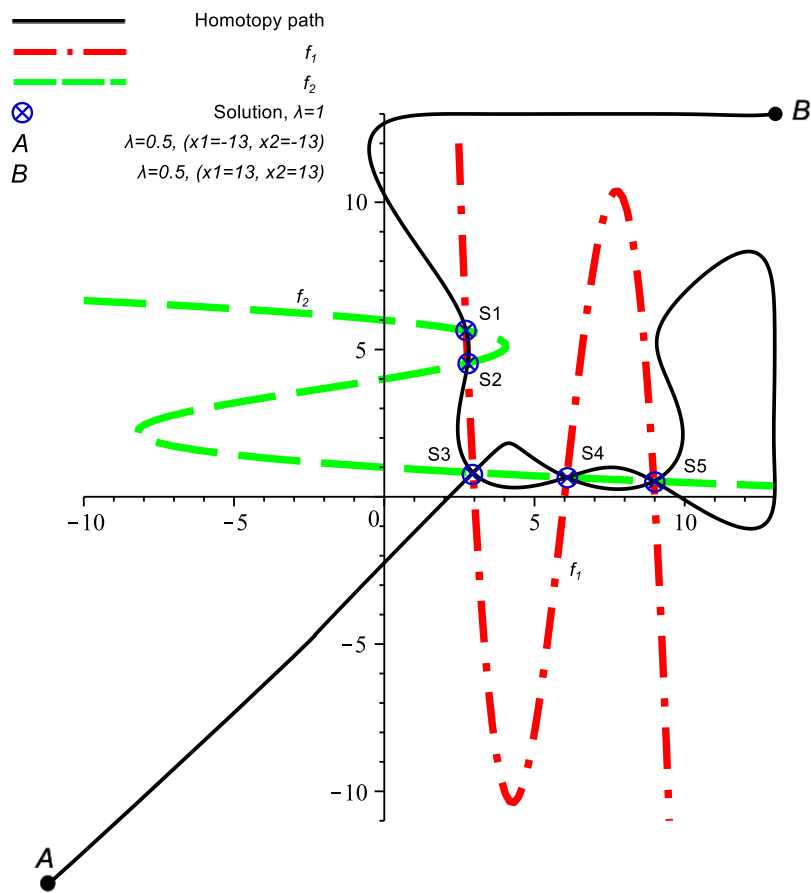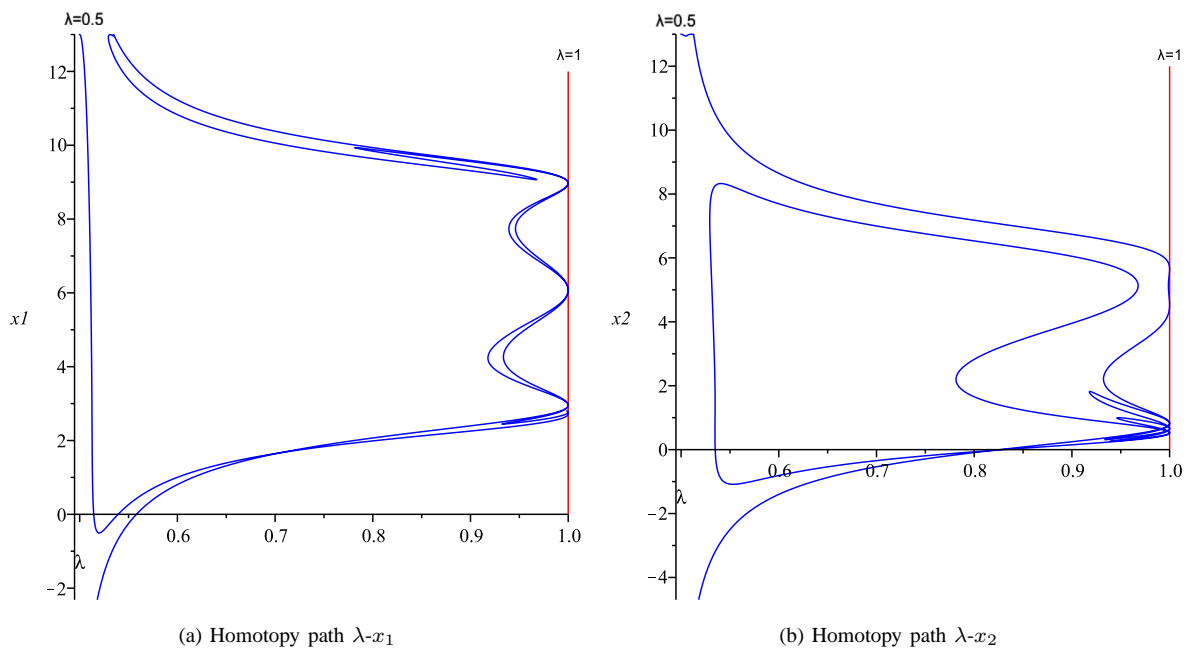
Fig. 12: Homotopy path for the 2 variable example.

(a) Homotopy path λ-x_1

(b) Homotopy path λ-x_2

Fig. 13: Homotopy paths.

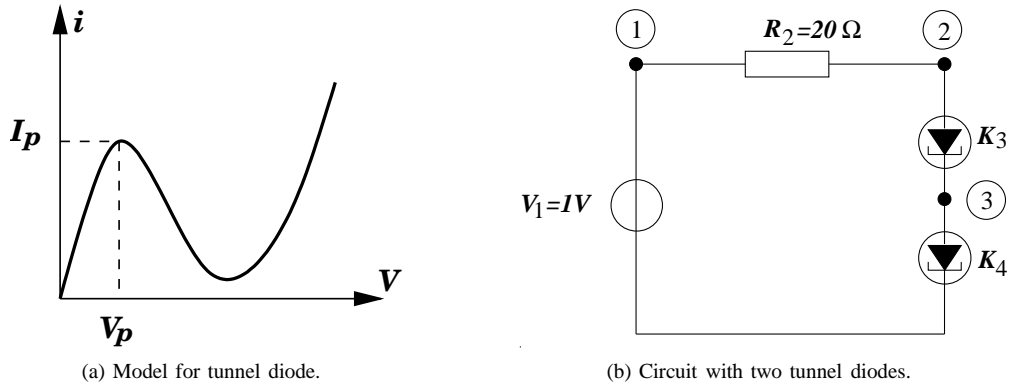(a) Model for tunnel diode.

(b) Circuit with two tunnel diodes.

Fig. 14: Tunnel diode study case.

C. Circuit with bipolar transistors and a diode

A circuit with bipolar transistors and a diode was reported in [16] and [20], it was solved using piecewise methods. Then, in [21], the circuit was resolved using modified fixed point Homotopy. This circuit has 3 operating points. The Ebers-Moll is used for all the transistors. The equation for the model is given as:

$$\left[\begin{array}{c} i_{D_E} \\ i_{D_C} \end{array} \right] = \left[\begin{array}{cc} 1 & \alpha_R \\ \alpha_F & 1 \end{array} \right] \left[\begin{array}{c} 10^{-9}(e^{(40 v_{be})} - 1) \\ 10^{-9}(e^{(40 v_{bc})} - 1) \end{array} \right]$$

The circuital rendering of the model is shown in figure 17.

As for the diode, the model is:

$$i_d = 10^{-9}(e^{40u} - 1)$$

The values for the circuit components can be found in table II. First, the equilibrium equation is formulated using the modified nodal analysis with the result of a system having 14 equations and 14 variables. The circuit is shown in figure 16 and the equilibrium equation es 10 (using MNA circuital analysis).

Component	Value
R_1	$4K\Omega$
R_2	$0.1K\Omega$
R_3	$8K\Omega$
R_4	$8K\Omega$
R_5	$4K\Omega$
R_6	$0.1K\Omega$
R_7	$30K\Omega$
R_8	$1K\Omega$
R_9	$0.1K\Omega$
R_{10}	$10K\Omega$
R_{11}	$4K\Omega$
R_{12}	$10K\Omega$
R_{13}	$1K\Omega$
V_{cc}	$12V$

TABLE II: Circuit components and values.

$$
\begin{array}{ll}
f_1 & \frac{37}{20000} v_1 - \frac{1}{4000} v_2 - \frac{1}{4000} v_6 - \frac{1}{1000} v_9 - \frac{1}{4000} v_{12} - \frac{1}{10000} v_{13} + IE = 0 \\
f_2 & -\frac{1}{4000} v_1 + \frac{3}{8000} v_2 - \frac{1}{8000} v_5 + 0.00000000990\, e^{40\, v_4 - 40\, v_3} + 0.00000000010 - 0.000000010\, e^{40\, v_4 - 40\, v_2} = 0 \\
f_3 & \frac{1}{100} v_3 - 0.000000010\, e^{40\, v_4 - 40\, v_3} + 0.00000000990 + 0.00000000010\, e^{40\, v_4 - 40\, v_2} = 0 \\
f_4 & \frac{1}{8000} v_4 - \frac{1}{8000} v_6 + 0.00000000010\, e^{40\, v_4 - 40\, v_3} - 0.00000001000 + 0.00000000990\, e^{40\, v_4 - 40\, v_2} = 0 \\
f_5 & -\frac{1}{8000} v_2 + \frac{1}{8000} v_5 + 0.00000000010\, e^{40\, v_5 - 40\, v_7} - 0.00000001000 + 0.00000000990\, e^{40\, v_5 - 40\, v_6} = 0 \\
f_6 & -\frac{1}{4000} v_1 - \frac{1}{8000} v_4 + \frac{3}{8000} v_6 + 0.00000000990\, e^{40\, v_5 - 40\, v_7} + 0.00000001010 - 0.000000010\, e^{40\, v_5 - 40\, v_6} - 0.000000010\, e^{40\, v_8 - 40\, v_6} = 0 \\
f_7 & \frac{1}{100} v_7 - 0.000000010\, e^{40\, v_5 - 40\, v_7} + 0.00000000990 + 0.00000000010\, e^{40\, v_5 - 40\, v_6} = 0 \\
f_8 & \frac{1}{30000} v_8 - \frac{1}{30000} v_9 + 0.000000010\, e^{40\, v_8 - 40\, v_6} - 0.000000010 = 0 \\
f_9 & -\frac{1}{1000} v_1 - \frac{1}{30000} v_8 + \frac{31}{30000} v_9 + 0.00000000990\, e^{40\, v_{11} - 40\, v_{10}} - 0.000000010\, e^{40\, v_{11} - 40\, v_9} = 0 \\
f_{10} & \frac{1}{100} v_{10} - 0.000000010\, e^{40\, v_{11} - 40\, v_{10}} + 0.00000000990 + 0.00000000010\, e^{40\, v_{11} - 40\, v_9} = 0 \\
f_{11} & \frac{1}{10000} v_{11} - \frac{1}{10000} v_{12} + 0.00000000010\, e^{40\, v_{11} - 40\, v_{10}} - 0.00000001000 + 0.00000000990\, e^{40\, v_{11} - 40\, v_9} = 0 \\
f_{12} & -\frac{1}{4000} v_1 - \frac{1}{10000} v_{11} + \frac{7}{20000} v_{12} + 0.00000000990\, e^{40\, v_{13}} + 0.00000000010 - 0.000000010\, e^{40\, v_{13} - 40\, v_{12}} = 0 \\
f_{13} & -\frac{1}{10000} v_1 + \frac{11}{10000} v_{13} + 0.00000000010\, e^{40\, v_{13}} - 0.00000001000 + 0.00000000990\, e^{40\, v_{13} - 40\, v_{12}} = 0 \\
f_{14} & v_1 - 12 = 0
\end{array}
\tag{10}
$$

Now, DBH is applied to solve the circuit; the Homotopy formulation is expressed as follows:

Point	v_1	v_2	v_3	v_4	v_5	v_6	v_7	v_8	v_9	v_{10}	v_{11}	v_{12}	v_{13}	i_E
Initial	+13	-13	+13	-13	-13	-13	-13	-13	-13	-13	-13	-13	-13	-13
Final	+13	+13	+13	+13	-13	+13	-13	+13	+13	+13	+13	+13	+13	+13

TABLE III: Initial point and final point.

Sol	v_1	v_2	v_3	v_4	v_5	v_6	v_7	v_8	v_9	v_{10}	v_{11}	v_{12}	v_{13}	i_E
S_1	12	5.995	0.085	0.368	0.712	0.436	0.390	0.699	11.635	0.4e-5	0.039	0.039	0.321	-0.0089
S_2	12	0.883	0.278	0.590	0.631	0.812	0.315	1.074	11.647	0.4e-5	0.039	0.039	0.321	-0.0100
S_3	12	0.405	0.366	0.685	0.349	6.796	0.070	7.038	11.839	0.4e-5	0.039	0.039	0.321	-0.0085

TABLE IV: Solutions for the circuit with bipolar transistors and a diode.

$$H_1(f_1, \lambda) = \lambda(\lambda + 1)(\lambda - 1)(\lambda - 2)(v_1 - 13)(v_1 + 13) + C(\lambda - 0.5)^2 f_1^2 = 0$$
$$H_2(f_2, \lambda) = \lambda(\lambda + 1)(\lambda - 1)(\lambda - 2)(v_2 - 13)(v_2 + 13) + C(\lambda - 0.5)^2 f_2^2 = 0$$
$$\vdots$$
$$H_{14}(f_{14}, \lambda) = \lambda(\lambda + 1)(\lambda - 1)(\lambda - 2)(I_E - 13)(I_E + 13) + C(\lambda - 0.5)^2 f_{14}^2 = 0$$

where the constant value $C = 0.000001$, the bounding lines are $a = 0$ and $b = 1$, and the initial point for the Homotopy path is selected as shown in table III.

So, the next step is to solve the circuit using the double bounded Homotopy, resulting in the convergence to the three known solutions for the circuit. The Homotopy path correspondent to the current of the voltage source I_E is displayed in figure 18. Finally, the final point for the Homotopy trace is exhibited in table III.

D. Chua's Circuit

Chua's circuit [17] (see figura 19), with 9 solutions, has become in the reference circuit for Homotopy applied to circuit analysis. The values for the components are shown in table V. This circuit has 4 bipolar transistors modeled by the Ebers-Moll model for the bipolar transistor operating in the direct active region (see figure 20).

Component	Value	Component	Value
R_1	$1k\Omega$	R_9	$10.1k\Omega$
R_2	$4k\Omega$	R_{10}	$10.1k\Omega$
R_3	$4k\Omega$	R_{11}	$4k\Omega$
R_4	$5k\Omega$	R_{12}	$4k\Omega$
R_5	$30k\Omega$	R_{13}	$30k\Omega$
R_6	$0.5k\Omega$	R_{14}	$30k\Omega$
R_7	$0.5k\Omega$	V_1	$10V$
R_8	$30k\Omega$	V_2	$2V$
V_{CC}	$12V$	α	0.98

TABLE V: Component values for Chua's circuit.

The resulting equation system is:

$$f_1 = 4.3663v_2 + 0.6103168 \times 10^{-5} e^{(40v_1)} - 12$$
$$+0.2863168 \times 10^{-5} e^{(40v_2)} = 0$$

$$f_2 = 5.4v_1 + v_3 + 0.3580 \times 10^{-5} e^{(40v_1)} - 22$$
$$+7 \times 10^{-7} e^{(40v_3)} + 5 \times 10^{-7} e^{(40v_4)} + 0.6620 \times 10^{-5} e^{(40v_2)} = 0$$

$$f_3 = 4.3663v_4 + 0.6103168 \times 10^{-5} e^{(40v_3)} - 12$$
$$+0.2863168 \times 10^{-5} e^{(40v_4)} = 0$$

Now, the DBH is applied to solve the circuit. The Homotopy formulation is expressed as:

$$H_1(f_1, \lambda) = \lambda(\lambda + 1)(\lambda - 1)(\lambda - 2)(v_1 - 10)(v_1 + 10) + (\lambda - 0.5)^2 f_1^2 = 0$$
$$H_2(f_2, \lambda) = \lambda(\lambda + 1)(\lambda - 1)(\lambda - 2)(v_2 - 10)(v_2 + 10) + (\lambda - 0.5)^2 f_2^2 = 0$$
$$H_3(f_3, \lambda) = \lambda(\lambda + 1)(\lambda - 1)(\lambda - 2)(v_3 - 10)(v_3 + 10) + (\lambda - 0.5)^2 f_3^2 = 0$$
$$H_4(f_4, \lambda) = \lambda(\lambda + 1)(\lambda - 1)(\lambda - 2)(v_4 - 10)(v_4 + 10) + (\lambda - 0.5)^2 f_3^2 = 0$$

where the bounding lines are $a = 0$ and $b = 1$, and the initial point for the Homotopy path es selected at $A = [v_1 = 10, v_2 = 10, v_3 = 10, v_4 = 10]$.

Equilibrium equation is the same as employed in [17]. The variables to be solved are branch voltages: v_1, v_2, v_3, and v_4. Figure 21 shows the Homotopy path for the branch voltage v_1. The final point for the path was $B = [v_1 = -10, v_2 = 10, v_3 = 10, v_4 = 10]$. Finally, the Homotopy was able to find 2 out of 9 solutions. The remaining 7 roots were isolated in one or more separate paths.

Found solutions are:

$$
\begin{bmatrix} v_1 \\ v_2 \\ v_3 \\ v_4 \end{bmatrix} = \underbrace{\begin{bmatrix} 0.3300 \\ 0.3680 \\ 0.3367 \\ 0.3642 \end{bmatrix}}_{\text{Solution } \textcircled{1}}, \underbrace{\begin{bmatrix} -0.7119 \\ 0.3775 \\ 0.3350 \\ 0.3653 \end{bmatrix}}_{\text{Solution } \textcircled{2}},
$$

V. CONCLUSIONS

The stop criterion for Homotopy methods consist in using a maximum number (arbitrarily number) of integration steps, in such a way that when integration steps reach the solution line the algorithm stops. Nevertheless, this kind of method may leave some roots out. A set of properties fo the PDA4 Homotopy were explained and developed. The bounded Homotopy with four solution lines shows interesting properties given by the fact that allows the Homotopy path to be placed between two limits named bounding lines. Also, the curvature radius on the solutions shows a proportional relationship with the separation between solution lines. Additionally, the curvature radius on the turning points of the solutions spatially matches with the critical points of the equilibrium equation and is directly proportional to $f(x)$ evaluated at the return. Another fundamental property of this new Homotopy is to possess a symmetry axis, which is found between solution lines ($\lambda = 0$ and $\lambda = a$), allowing the implementation for a stop criterion. Finally, bounded Homotopy with 4 solution lines was applied to DC simulations for some circuit examples and to a mathematical example, showing its potential to be used on non-linear circuit analysis.

REFERENCES

[1] *Star-hspice manual*, (1998), 6–1.
[2] *Affirma spectre circuit simulator user guide*, (2000), 17.
[3] *Aplac manual: Dc analysis*, (2004).
[4] J. E. Dennis and Jorge J. Moré, *Quasi-Newton methods, motivation and theory*, Siam Review **19** (1977), no. 1.
[5] Mollick E., *Establishing moore's law*, Annals of the History of Computing **28** (2006), no. 3, 62–75.
[6] M. M. Green, *An efficient continuation method for use in globally convergent dc circuit simulation*, ISSSE Proceedings (1995), 497–500.
[7] S.H. Jen, B.J. Sheu, and Y. Oshima, *A unified approach to submicron dc mos transistor modeling for low-voltage ics*, Analog Integrated Circuits and Signal Processing **12** (1997), 107–118.
[8] LTspice, *Version iv*, Linear Techonology, Milpitas, CA, USA.
[9] R. C. Melville and L. Trajković, *Artificial parameter homotopy methods for the dc operating point problem*, IEEE transactions on computer-aided design of integrated circuits and systems **12** (1997), no. 6, 861–877.
[10] J. Ogrodzki, *Circuit simulation: methods and algorithms*, (1994).
[11] Roychowdhury and R. J. Melville, *Delivering global dc convergence for large mixed-signal circuits via homotopy/continuation methods*, IEEE Transactions on Computer-Aided Design of Integrated Circuits and Systems **25** (2006), no. 1, 66.
[12] Chung-Wen Ho Ruehli and P. A. Brennan, *The modified nodal approach to network analysis*, IEEE Transactions on Circuits and Systems **22** (1975), no. 6, 504.
[13] A. F. Schwarz, *Computer-aided design of microelectronic circuits and systems: Volume 1*, (1987), ISBN 0-12-632431-X.
[14] M. Shur, *Introduction to electronic devices*, (1996).
[15] S. M. Sze, *Semiconductor devices: Physics and technology*, (1985).
[16] M. Tadeusiewicz and K. Glowienka, *A contraction algorithm for finding all the dc solutions of piecewise-linear circuits*, J. Circuits, Syst. Comput. **4** (1994), 319–336.
[17] A. Ushida and L. O. Chua, *Tracing solution curves of non-linear equations with sharp turning points*, Circuit Theory and Applications **12** (1984), 1–21.
[18] A. Ushida, Y. Yamagami, I. Kinouchi, Y. Nishio, and Y. Inoue, *An efficient algorithm for finding multiple dc solutions based on the spice-oriented newton homotopy method*, IEEE Transactions on Computer-Aided Design of Integrated Circuits and Systems **21** (2002), no. 3, 337–348.
[19] D. M. Wolf and S. R. Sanders, *Multiparameter homotopy methods for finding dc operating points of nonlinear circuits*, IEEE transactions on circuits and systems-I: fundamental theory and aplications **43** (1996), no. 10, 824–837.
[20] K. Yamamura and T. Ohshima, *Finding all solutions of piecewise-linear resistive circuits using linear programming*, IEEE transactions on circuits and systems-I: fundamental theory and aplications **45** (1998), 434–445.
[21] K. Yamamura, T. Sekiguchi, and Y. Inuoe, *A fixed-point homotopy method for solving modified nodal equations*, IEEE transactions on circuits and systems-I: fundamental theory and aplications **46** (1999), no. 6, 654–664.
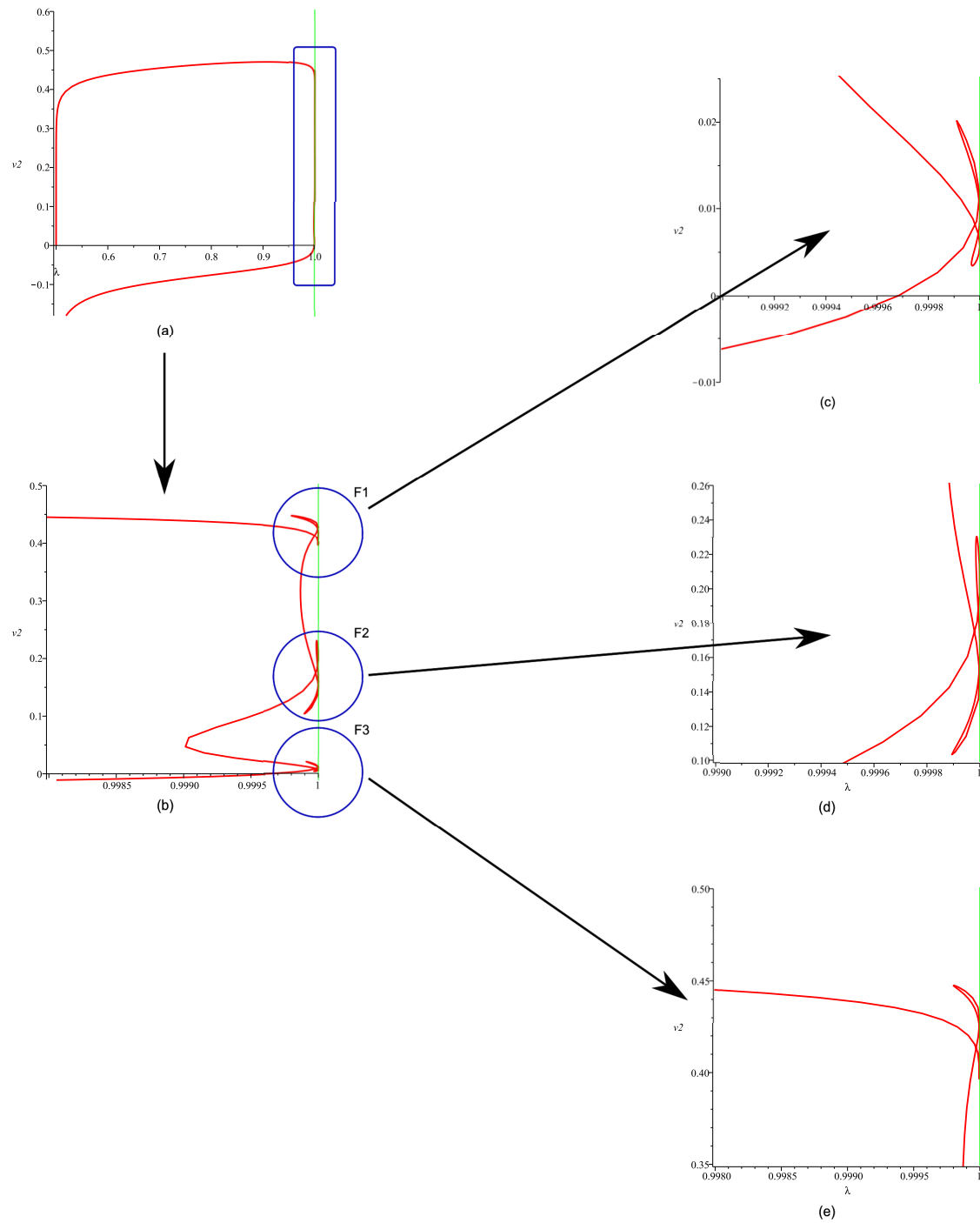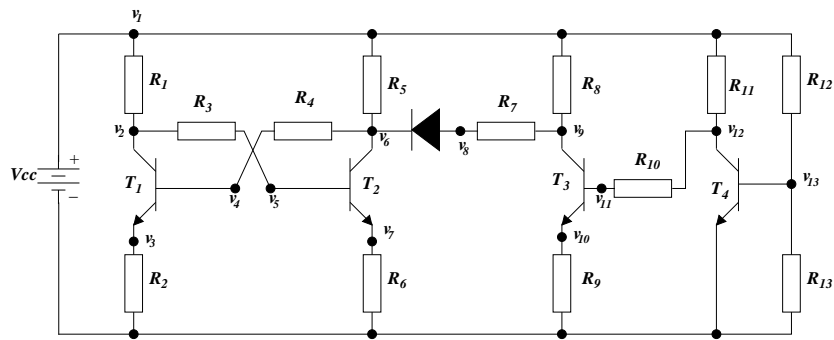
Fig. 15: Homotopy path for the circuit with tunnel diodes.
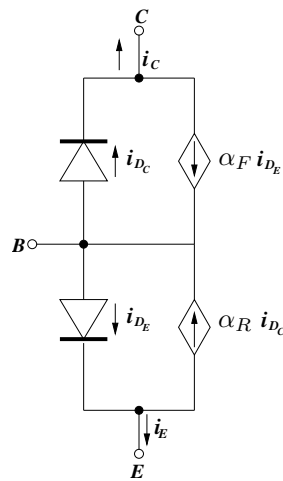
Fig. 16: Circuit with bipolar transistors and a diode.
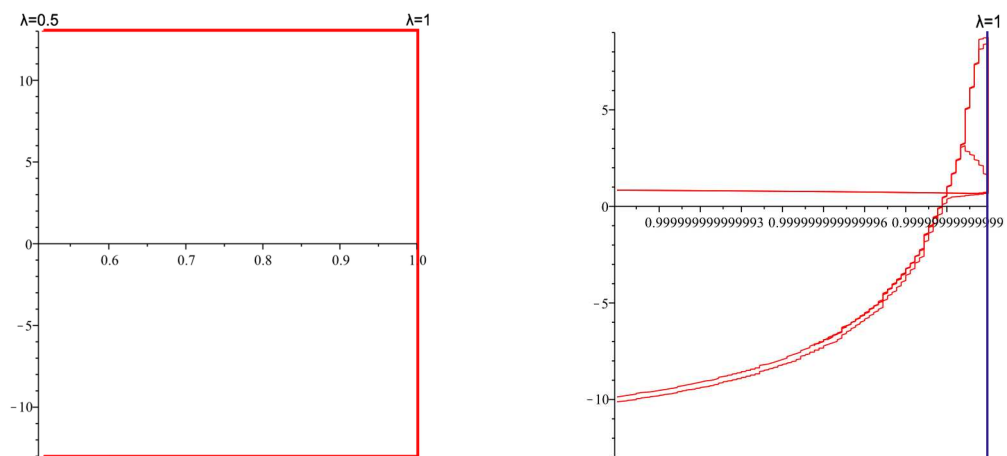

Fig. 17: Ebers-Moll model for bipolar transistor.

Fig. 18: Homotopy path $\lambda - v_8$.
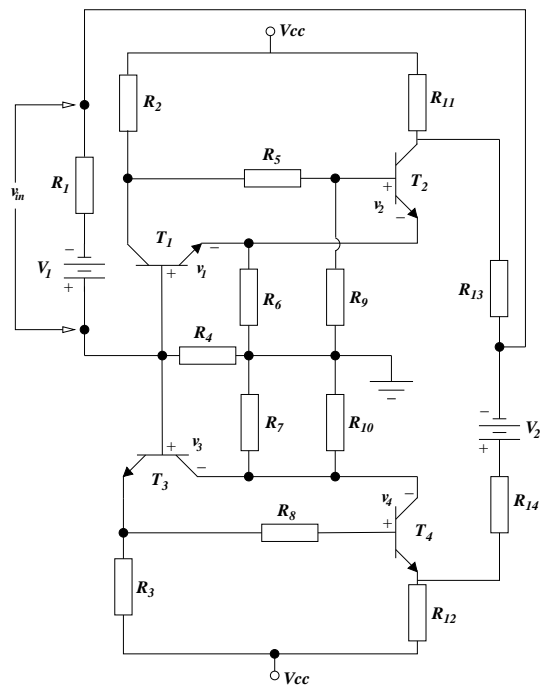
Fig. 19: Chua's circuit with 9 solutions.

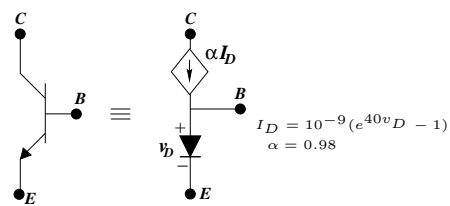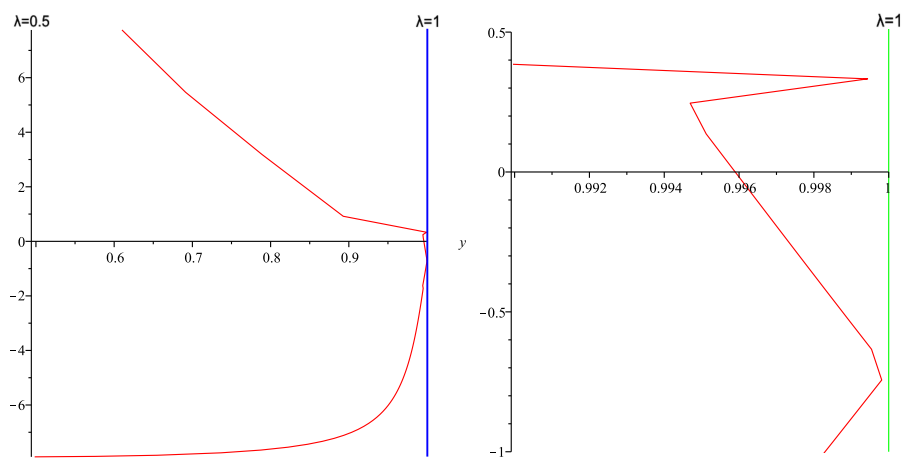$$I_D = 10^{-9}(e^{40v_D} - 1)$$
$$\alpha = 0.98$$

Fig. 20: Half-side Ebers-Moll model.

Fig. 21: Chua's circuit solution.